

# Sub-solidus melting of directionally solidified Rene 80 superalloy during solution heat treatment

R. K. Sidhu · O. A. Ojo · M. C. Chaturvedi

Received: 18 September 2007 / Accepted: 26 February 2008 / Published online: 23 March 2008  
© Springer Science+Business Media, LLC 2008

**Abstract** The microstructure of directionally solidified Rene 80 (DS Rene 80) superalloy in the standard solution heat treated condition was examined. Sub-solidus incipient melting was observed, which was found to be caused by the liquation of terminal solidification reaction products present in front of the  $\gamma$ - $\gamma'$  eutectic in the as-cast alloy. Based on the differential scanning calorimetry (DSC) measurements, and microstructural examination of heat-treated and water-quenched specimens, sub-solidus incipient melting in the alloy is likely to occur below 1,160 °C, and this is a key factor to be considered in the development of a suitable solution heat treatment scheme for DS Rene 80.

## Introduction

Rene 80<sup>1</sup> is a cast, nickel-based superalloy commonly used to manufacture first and second stage turbine blades in modern jet engines. It possesses an excellent combination of high rupture strength, thermal fatigue and hot corrosion resistance [1]. Directional solidification of the alloy results in a marked improvement in its mechanical properties as tensile strength is increased by about 10–15% and the creep-rupture life is extended by 2–4 times, as compared to the conventionally cast material [2, 3]. The high-temperature strength of the alloy is primarily derived from precipitation hardening by ordered L1<sub>2</sub> intermetallic Ni<sub>3</sub>(Al,Ti)  $\gamma'$  phase. The two major techniques to optimize the properties of most  $\gamma'$  strengthened superalloys are the

addition of various alloying elements and the use of suitable heat treatments to control the size and morphology of the  $\gamma'$  particles [4].

In complex casting alloys such as Rene 80, which contain a rather high concentration of alloying elements, there could be a significant variation in the nature of  $\gamma'$  particles due to the effects of dendritic microsegregation and cooling rate during ingot solidification, which is particularly slow in a directional solidification process. This results in the formation of smaller  $\gamma'$  particles in the dendrite cores and coarser  $\gamma'$  particles and  $\gamma$ - $\gamma'$  eutectic constituent in the interdendritic regions. To dissolve all the primary  $\gamma'$  particles and homogenize the as-cast alloy to subsequently achieve a uniform distribution of re-precipitated fine  $\gamma'$  particles for better creep-rupture properties, the solution heat treatment needs to be done in the single phase ( $\gamma$ ) field above the  $\gamma'$  solvus temperature but below the solidus temperature. However, it has been observed that the upper limit for the homogenization or solution heat treatment temperature in many polycrystalline (equiaxed) and columnar grain directionally solidified (CGDS) nickel-base superalloys is limited by the problem of incipient melting [5–7]. Despite the fact that it may have very important implications for the high-temperature mechanical properties as well as the weldability, incipient melting during heat treatment has not been reported so far in this alloy. Therefore, the aim of the present study was to investigate the occurrence of incipient melting in this alloy, which could aid the development of improved solution heat treatment scheme for the material.

R. K. Sidhu (✉) · O. A. Ojo · M. C. Chaturvedi  
Department of Mechanical and Manufacturing Engineering,  
University of Manitoba, Winnipeg, MB, Canada R3T 5V6  
e-mail: sidhurk@cc.umanitoba.ca

<sup>1</sup> Rene 80 is a trademark of GE (General Electric Co. USA).

## Experimental procedure

Directionally solidified Rene 80 (DS Rene 80) alloy of nominal composition (wt%) 3.0 Al, 5.0 Ti, 9.5 Co, 14.0 Cr, 4.0 Mo, 4.0 W, 0.17 C, 0.015 B, 0.03 Zr was remelted and directionally solidified in a Bridgman furnace in the form of bars of size  $75 \times 25 \times 6$  mm. Controlled uniaxial heat flow during directional solidification process resulted in the formation of an oriented columnar grain structure with grains aligned parallel to a preferred crystallographic direction (as opposed to the equiaxed microstructure of the conventionally cast alloy). In case of face centred cubic (fcc) nickel-based alloys like DS Rene 80, this preferred direction is  $\langle 001 \rangle$  direction, which is aligned parallel to the solidification axis of the cast material. Specimens of size  $10 \times 10 \times 6$  mm were sectioned from the as-cast DS material by electro-discharge machining (EDM) and solution heat treated at  $1,204^\circ\text{C}$  for 2 h in an argon atmosphere, using a heating rate of  $10^\circ\text{C}/\text{min}$ . to  $1,100^\circ\text{C}$  and  $2.5^\circ\text{C}/\text{min}$ . from  $1,100$  to  $1,204^\circ\text{C}$ .

Specimens were prepared by standard metallographic techniques and electrolytically etched in a solution of  $12\text{ mL H}_3\text{PO}_4 + 40\text{ mL HNO}_3 + 48\text{ mL H}_2\text{SO}_4$  at 6 V for 5 s. The microstructure was examined by an optical microscope and a JEOL-5900 scanning electron microscope (SEM) equipped with an ultra-thin window Oxford energy dispersive X-ray spectrometer (EDS) system. A Netzch-404C differential scanning calorimeter (DSC) was used to study the solidification behaviour of the alloy. The measurements were carried out in an argon atmosphere at a heating and cooling rate of  $2.5^\circ\text{C}/\text{min}$ .

## Results and discussion

The as-cast microstructure of the DS Rene 80 alloy is shown in Fig. 1a and b. The cored dendritic microstructure due to the microsegregation that occurred in the alloy during solidification is illustrated in the backscattered electron image in Fig. 1a. EDS analysis of the different regions indicated that the elements Ti, Ta, Zr and Mo segregated to the interdendritic regions and their concentration was lowest in the centre of the dendrite cores. Conversely, the concentration of W, Co and Ni was measured to be higher in the cores than that observed in the interdendritic regions. Similar segregation behaviour has been reported in the literature in other nickel-based superalloys [8].

The size and the morphology of  $\gamma'$  particles were observed to vary considerably from the dendrite core to the interdendritic regions (Fig. 1b).  $\gamma'$  particles in the dendrite cores varied from smaller ‘ogdoadically diced cubes’ to nearly rounded cuboidal particles of size  $0.3\text{--}0.4\ \mu\text{m}$ ,

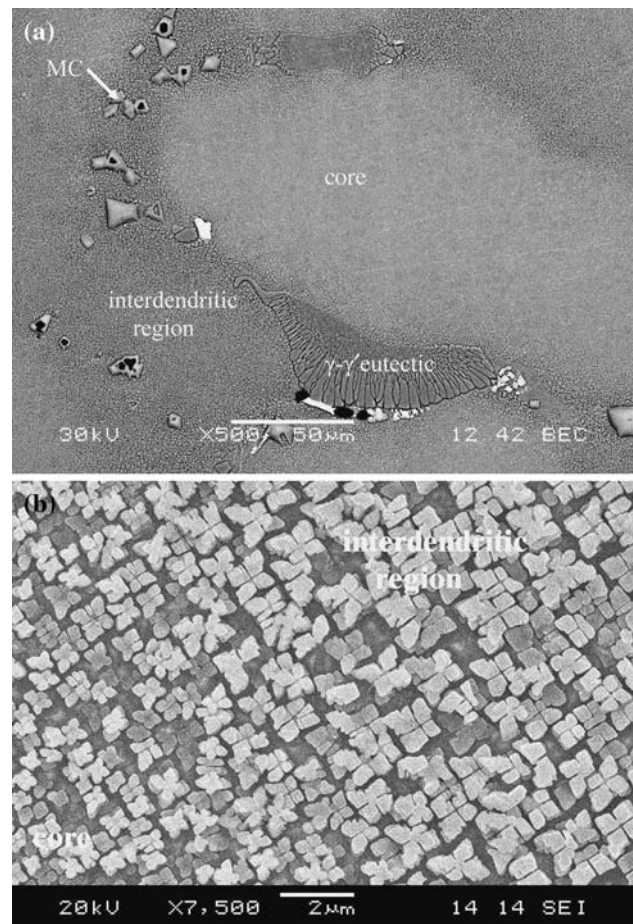


**Fig. 1** Microstructure of the as-cast alloy (a) SEM backscattered electron image showing a cored dendritic microstructure (b) SEM secondary electron image showing variation in the size of  $\gamma'$  particles in different regions

whereas the interdendritic regions contained coarser  $\gamma'$  particles in the form of ‘ogdoadically diced cube clusters’ of size  $0.6\text{--}0.9\ \mu\text{m}$  (Fig. 1b). Other secondary solidification constituents such as Ti-rich MC carbides and  $\gamma\text{--}\gamma'$  eutectic formed during solidification were also present within the interdendritic regions (Fig. 1a). In addition, the occurrence of a different eutectic-type microconstituent was noticed in front of many  $\gamma\text{--}\gamma'$  eutectic cells, which is shown in the atomic number contrast-based backscattered electron image in Fig. 2a. The lamellar morphology of this product indicates that it is formed by eutectic transformation involving either ternary or quaternary eutectic reactions. Microchemical analysis of different constituent phases present in this eutectic-like solidification product by energy dispersive X-ray microanalysis showed that the two major phases observed in Fig. 2a were rich in elements Ni, Zr and Ni, Ti, as shown in EDS spectra given in Fig. 2b and c, respectively. The chemical composition of these phases, given in Table 1, suggests that they were based on intermetallics  $\text{Ni}_5\text{Zr}$  and  $\text{Ni}_3\text{Ti}$ . A significant concentration

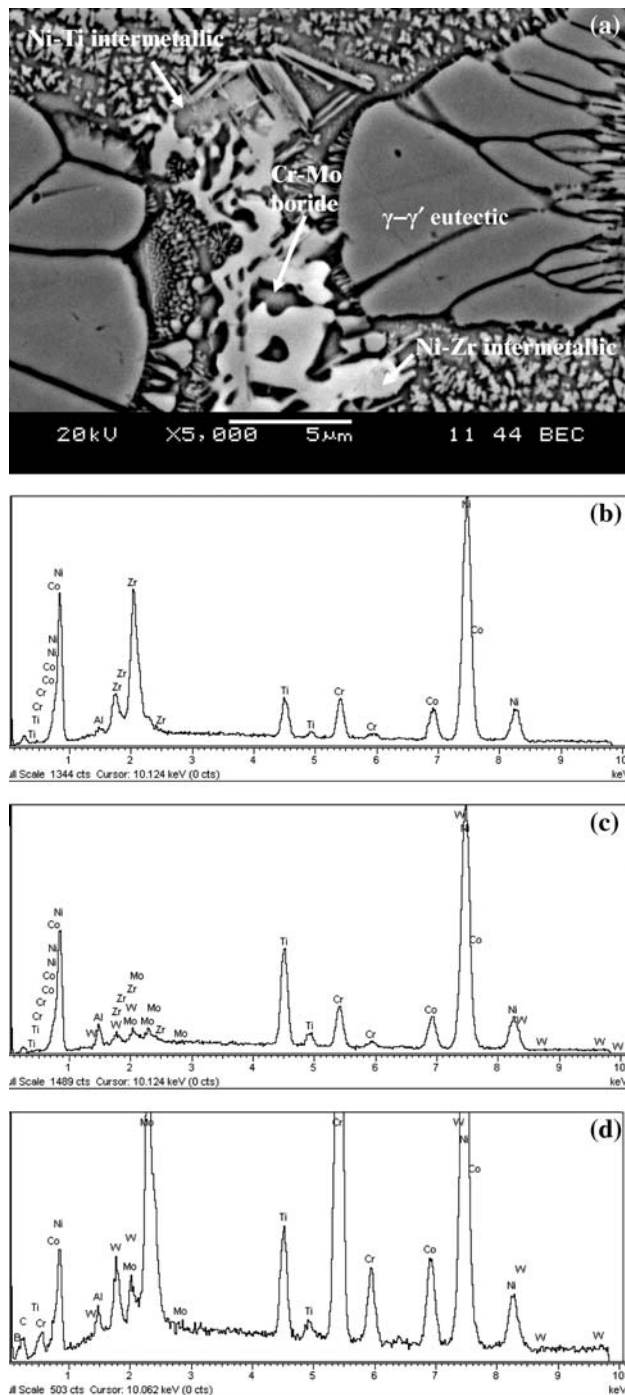


**Fig. 2** (a) SEM backscattered electron image of the as-cast alloy showing eutectic-like constituent ahead of  $\gamma$ - $\gamma'$  eutectic and EDS spectra from (b) Ni-Zr intermetallic (c) Ni-Ti intermetallic and (d) Cr-Mo boride

of boron was detected by the ultra-thin window EDS detector in particles of another phase, which also had a high concentration of Cr and Mo (Fig. 2d). High Cr and Mo peaks observed in the EDS spectra in this work (Fig. 2d) are the characteristic features of the boride ( $M_3B_2/M_5B_3$ ) phase observed in many nickel-base

**Table 1** EDS analyses of terminal solidification constituents (at.%)

Element	Ni-Zr intermetallic	Ni-Ti intermetallic	Cr-Mo boride
Al	1.5	3.9	–
Ti	4.8	12.2	4.1
Cr	5.8	6.0	57.4
Co	7.6	7.7	3.5
Ni	66.9	67.8	11.1
Zr	13.4	1.0	–
Mo	–	0.9	22.2
W	–	0.6	1.8

superalloys [9, 10]. Presence of boride particles in Rene 80 is also reported by other researchers [11, 12].

Solution heat treatment at 1,204 °C for 2 h, which is the standard solution heat treatment reported for both directionally solidified [2] and conventionally cast Rene 80 [12], resulted in dissolution of almost all the primary  $\gamma'$  particles in the cores and the interdendritic regions. The microstructure after this heat treatment, shown in Fig. 3a, therefore, mainly consisted of fine spheroidal secondary  $\gamma'$  particles of  $\sim 0.1 \mu\text{m}$  size dispersed uniformly in the matrix (inset in Fig. 3a), which formed during cooling from the solution treatment temperature. However, it was observed in the present study, that though this heat treatment (1,204 °C/2 h) was able to dissolve the primary  $\gamma'$  particles in the cores as well as the interdendritic regions, the microstructure consisted of many incipiently melted islands, such as those shown in Fig. 3a. The constituent phases present in the incipiently melted region are clearly delineated in the higher magnification micrograph in Fig. 3b, which is an atomic number contrast-based back-scattered electron micrograph of the solution heat-treated alloy. Chemical analysis of various phases observed in many similar incipiently melted regions by EDS indicated the existence of Ni-Zr and Ni-Ti rich intermetallics, and Cr-Mo rich borides in them. The chemical composition of these phases was found to be comparable to similar products detected in the eutectic-like regions observed in front of the  $\gamma$ - $\gamma'$  eutectic cells in the as-cast alloy, shown in Fig. 2a.

The occurrence of incipient melting and the association of constituents such as Cr-Mo borides and Ni-Ti and Ni-Zr rich intermetallics with these regions in the solution-treated material can be understood from the partitioning behaviour of various alloying elements during solidification of similar precipitation-hardened nickel-based superalloys [8]. Figure 4a and b shows the DSC thermograms of the DS Rene 80 during heating and cooling at a constant rate of 2.5 °C/min. During heating (Fig. 4a), dissolution of the core and interdendritic  $\gamma'$  precipitates was observed to occur around 1,122 and 1,169 °C, respectively.



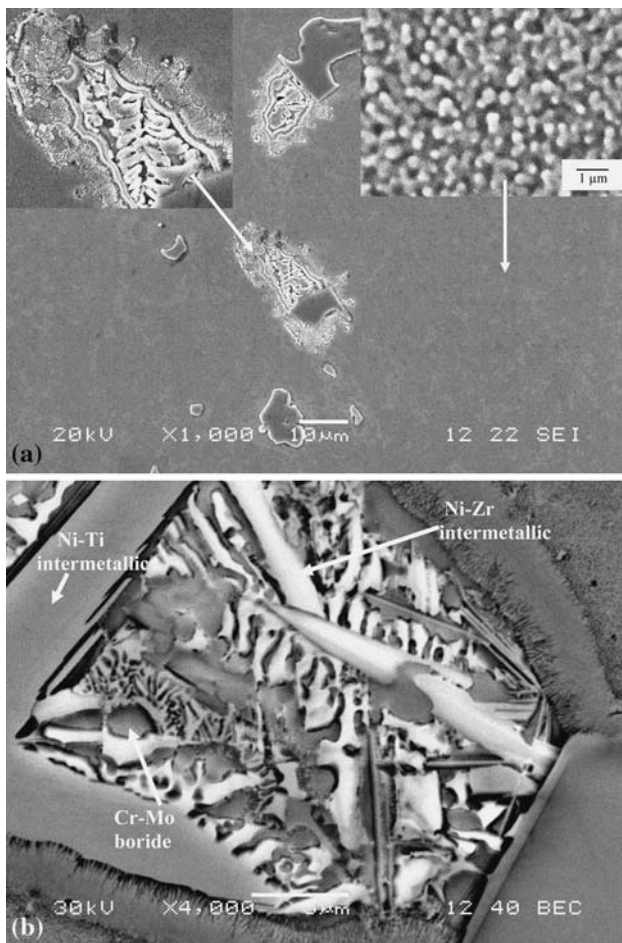


**Fig. 3** SEM micrographs of solution heat-treated (1,204 °C/2h/AC) alloy showing (a) regions of incipient melting and secondary  $\gamma'$  particles (inset) (b) backscattered electron image showing eutectic-like constituent in the incipient melting region at a higher magnification

The liquidus, solidus and  $\gamma'$  solvus temperatures measured during cooling (Fig. 4b) were observed to be 1,335, 1,264 and 1,141 °C, respectively, which are comparable to the values reported [13] for conventionally cast Rene 80 alloy.

In precipitation-hardened alloys like Rene 80, the first solid to form from the liquid during cooling is the  $\gamma$  dendrites. As these dendrites grow during subsequent cooling, dendritic microsegregation occurs with interdendritic liquid getting enriched with Ti and other carbide forming elements, which exhibit a partition coefficient  $k < 1$ , together with C atoms. Supersaturation of the liquid with these solutes due to continual enrichment on cooling would invariably result in the formation of secondary solidification constituents like MC carbides and  $\gamma$ - $\gamma'$  eutectic in the interdendritic regions. Formation of MC carbides and  $\gamma$ - $\gamma'$  eutectic in the present alloy was observed to occur around 1,280 and 1,186 °C, respectively. Further solute partitioning occurs during the formation of  $\gamma$ - $\gamma'$  eutectic involving

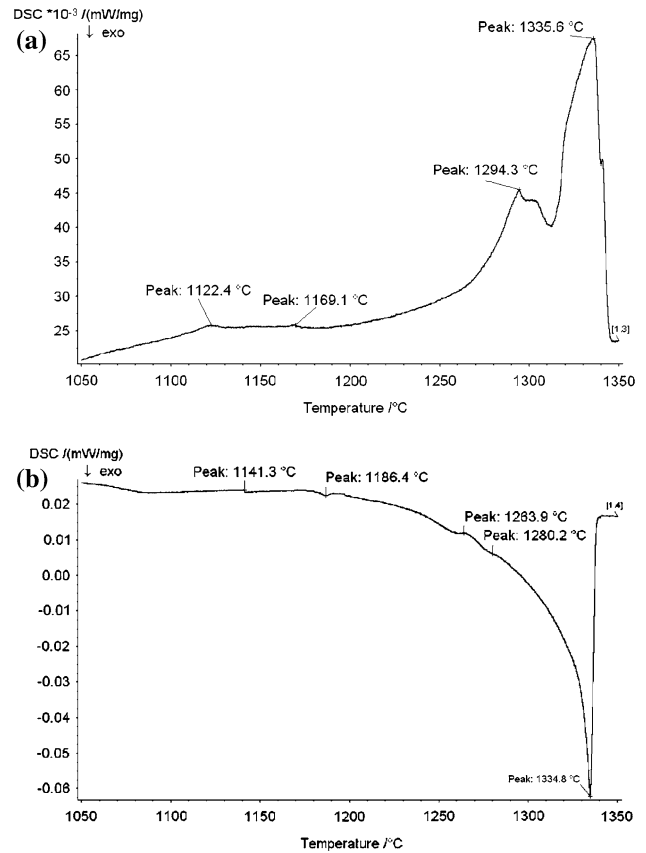


**Fig. 4** DSC thermograms for DS Rene 80 alloy during (a) heating (b) cooling

rejection of solute atoms with low solubility in  $\gamma$  and  $\gamma'$  phases into the residual liquid pool ahead of the formed  $\gamma$ - $\gamma'$  eutectic. In such a case, Zr and B, which have limited solubility in  $\gamma$  and  $\gamma'$  phases and exhibit severe positive segregation in nickel alloys, would preferentially segregate into the liquid phase. Moreover, considering the high affinity of Cr and Mo for B, these elements could also segregate into the residual liquid in front of  $\gamma$ - $\gamma'$  eutectic. Positive segregation of Cr and Mo into the residual liquid phase during  $\gamma$ - $\gamma'$  eutectic transformation in a nickel-base superalloy has also been reported by Zhu et al. [14]. Considering the positive segregation behaviour of Ti ( $k < 1$ ) versus the negative segregation behaviour of Al ( $k > 1$ ), the remaining liquid will be even further enriched with Ti. It is known that once the ratio of Ti/Al exceeds 3:1,  $\text{Ni}_3\text{Ti}$  would form preferentially, which could explain the formation of a  $\text{Ni}_3\text{Ti}$ -based intermetallic in the present work. On continuous cooling to the invariant freezing temperature for a given alloy composition, i.e., the effective solidus temperature, below which liquid phase could no longer exist, the remaining liquid would invariably complete solidification by terminal eutectic transformation, which may involve formation of multiple constituent phases. This would explain the presence of eutectic-like

products containing  $\gamma$  phase, Cr-Mo rich boride and Ni-Zr and Ni-Ti intermetallics, observed in this study.

Formation of  $\gamma$ - $\gamma'$  eutectic at around 1,186 °C in the DS Rene 80 alloy, and terminal solidification reaction product at much lower temperature, thus, support the occurrence of incipient melting during standard solution heat treatment of the alloy at 1,204 °C. Though dissolution of almost all the primary  $\gamma'$  precipitates was observed at 1,204°C, the alloy significantly suffered from sub-solidus incipient melting of the terminal solidification products (Fig. 3a and b). The melting temperature of the terminal solidification product was determined by heating the as-cast alloy in the range of 1,120–1,180 °C, holding at the desired temperature for 15 min, followed by water quenching to freeze the microstructure for subsequent metallographic examination. Incipient melting of the terminal solidification product was observed to occur at a temperature as low as 1,160 °C (Fig. 5a and b). The occurrence of incipient melting at 1,160 °C would, therefore, suggest that the upper limit for the heat treatment of this alloy should be less than

1,160 °C. However, it is seen in Fig. 5a and b, that many of the large  $\gamma'$  precipitates remained undissolved at this temperature. Overlap of the incipient melting region with the region where a certain amount of  $\gamma'$  precipitates remained undissolved is, therefore, the key factor to be considered for developing an appropriate solution heat treatment for DS Rene 80.

The occurrence of incipient melting is not only important in influencing the high-temperature mechanical properties of solution heat-treated DS Rene 80, but could also impair resistance of the material to HAZ liquation cracking during welding. It has been observed that liquation, which could occur by different mechanisms, is the primary cause of low HAZ crack resistance in most austenitic alloys, including precipitation-hardened nickel-base superalloys [15, 16]. A combination of thermally induced welding strain and very low ductility in the alloy due to localized melting at grain boundaries because of liquation of phases present on them results in HAZ liquation cracking. HAZ liquation is known to occur either by non-equilibrium interface melting below an alloy's solidus or by equilibrium super-solidus melting. Sub-solidus HAZ liquation, which includes melting of terminal solidification reaction products, is generally considered more detrimental to crack resistance as it extends the effective melting range of an alloy. In addition, it also influences the nature of super-solidus melting by pre-establishing non-equilibrium film at a lower temperature which alters the reaction kinetics during the subsequent heating. Therefore, proper consideration of terminal solidification microconstituents reported in this work, which can incipiently melt below 1,204 °C, would be prudent in the development of a suitable solution heat treatment to improve the mechanical properties as well as the HAZ cracking resistance of DS Rene 80 during welding. One possible method to eliminate or at least reduce the occurrence of incipient melting in this alloy could involve the use of an annealing heat treatment (at < 1,160 °C) to dissolve the terminal solidification constituents by solid state dissolution process prior to the presently used solution heat treatment at 1,204 °C.

**Acknowledgements** The authors would like to thank NSERC Canada and the consortium of Manitoba aerospace industries for financial support.

## References

1. Ross EW (1971) *Metal Prog* 99:93
2. Raguet M, Antolovich SD, Payne RK (1984) *Superalloys*. In: Gell M et al (eds) *Proceedings of the 5th international symposium on superalloys 1984*, Seven Springs, PA, USA, The Metallurgical Society, p 231
3. Nakagawa YG, Ohtomo A, Saiga Y (1976) *Trans Jpn Inst Met* 17:323

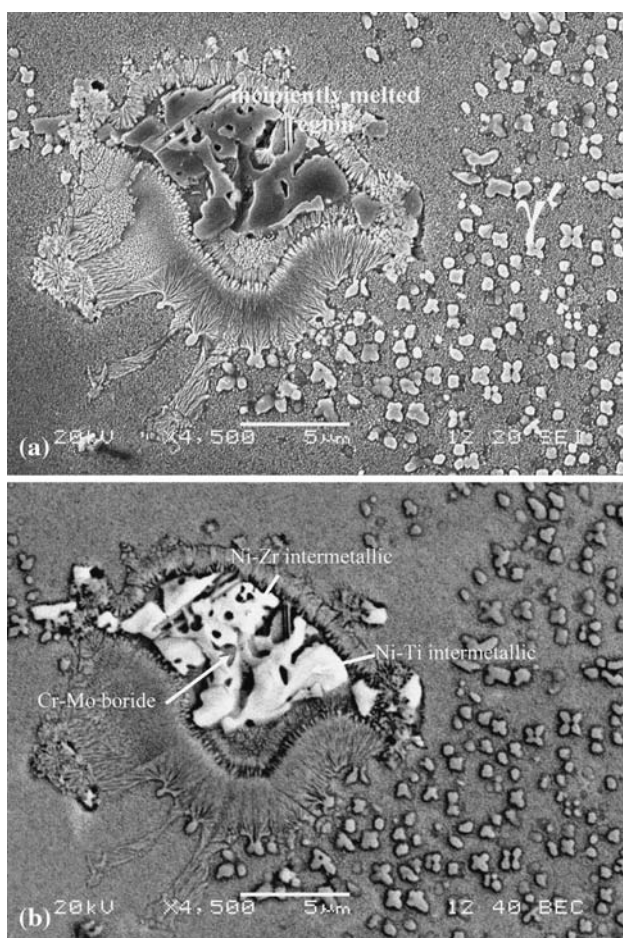


**Fig. 5** SEM micrographs showing the incipient melting region in as-cast sample heated to a peak temperature of 1,160 °C (a) secondary electron image (b) backscattered electron image

4. Nazmy M (1993) Proceedings of the conference on critical issues in the development of high temperature structural materials, March 7–14, Kona, HI, USA, p 321
5. Zheng Y, Cai Y, Wang L (1983) *Acta Met Sinica* 19:A190
6. Ojo OA, Richards NL, Chaturvedi MC (2004) *J Mater Sci Lett* 39:7401
7. Baldan A (1989) *Zeitschrift fur Metallkunde* 80:635
8. Zeisler-Mashl KL, Pletka BJ (1992) Superalloys. In: Antolovich SD, Stusrud RW, MacKay RA, Anton DL, Khan T, Kissinger RD, Klarstrom DL (eds) Proceedings of the 7th international symposium on superalloys, Seven Springs, PA, USA, The Minerals, Metals & Materials Society, p 175
9. Seo SM, Kim IS, Lee JH, Jo CY, Miyahara H, Ogi K (2007) *Met Mater Trans* 38A:883. doi:[10.1007/s11661-007-9090-0](https://doi.org/10.1007/s11661-007-9090-0)
10. Boesch WJ, Canada HB (1968) *J Metals* 20:46
11. Collins HE (1974) *Metall Trans* 5A:189
12. Safari J, Nategh S (2006) *J Mater Processing Technol* 176:240. doi:[10.1016/j.jmatprotec.2006.03.165](https://doi.org/10.1016/j.jmatprotec.2006.03.165)
13. Sponseller DL (1996) Superalloys. In: Kissinger RD, Deye DJ, Anton DL, Cetel AD, Nathal MV, Pollock TM, Woodford DA (eds) Proceedings of the 8th international symposium on superalloys, Seven Springs, PA, USA, The Minerals, Metals & Materials Society, p 259
14. Zhu Y, Zhang S, Xu L, Bi J, Hu Z, Shi C (1998) In: Reichman S, Duhl DN, Maurer G, Antolovich S, Lund C (eds) Proceedings of the 6th international symposium on superalloys, Seven Springs, PA, USA, 1988, The Metallurgical Society, p 703
15. Romig Jr D, Lippold JC, Cieslak ML (1988) *Metall Trans* 19A:35
16. Owczarski WA, Duvall DS, Sullivan CP (1966) *Weld J* 44:145